The Use of LIDAR to Characterize Aircraft Exhaust Plumes

Paper # 69965

Roger L. Wayson
University of Central Florida
Civil & Environmental Engineering
P.O. Box 162450
Orlando, FL 32816-2450

Gregg G. Fleming, Brian Kim
U.S. Department of Transportation
Research and Special Programs Administration
John A. Volpe National Transportation Systems Center
Environmental Measurement and Modeling Division, DTS-34
Air Quality Facility, Kendall Square
Cambridge, MA 02142-1093

Wynn L. Eberhard, W. Alan Brewer
National Oceanic and Atmospheric Administration
Environmental Technology Laboratory
Optical Remote Sensing Division
325 Broadway
Boulder, CO 80303

Julie Draper
Federal Aviation Administration
Office of Environment and Energy
800 Independence Ave., S.W.
Washington, DC 20591

John Pehrson
Camp Dresser & McKee Inc.
18581 Teller Ave., Suite 200
Irvine, CA 92612

Roger Johnson
Los Angeles World Airports
1 World Way
Los Angeles, CA 90045

ABSTRACT

Aircraft emissions are a growing concern for the FAA, airports, and the community. U.S. and international air quality models were previously unable to accurately predict initial plume dispersion and the resulting pollutant concentrations because the characteristics of the initial plume behavior were virtually unknown. These data are needed as input to dispersion models, such as the FAA's Emissions and Dispersion Modeling System (EDMS), for use in complying with air quality requirements. Since very little research had been done in this area, input values previously used were primarily based on the best available information and good engineering judgment. The Volpe National Transportation Systems Center, FAA's Office of Environment and Energy (AEE), the National Oceanic and Atmospheric Administration (NOAA), and the Los Angeles International Airport (LAX), teamed up to conduct a study of aerosol plume behavior from jet exhaust using **LI**ght **D**etection **A**nd **R**anging or LIDAR. LIDAR has been used for previous measurements to study wing-tip vortices and some pollutant evaluations near airports, and was concluded to be appropriate for this application. In support of AEE, the John A. Volpe National Transportation Systems Center initiated action to conduct the research. Volpe enlisted the assistance of the NOAA, based on their large amount of experience with LIDAR. NOAA has several LIDAR units and the flexibility to re-engineer the units and associated software on a project-by-project basis making them the perfect fit for this team. Setup and measurements occurred from May 14 through 24, 2001. The results of the measurements have exceeded expectations allowing quantification of aircraft plume rise and initial dispersion parameters (standard deviations) at this major urban airport. This paper will summarize the methodology, results and conclusion of this project.

INTRODUCTION

The goal of this study was to measure the initial plume characteristics of jet exhaust plumes. Cross-sections of the plume were measured at a variety of distances behind the aircraft during takeoff roll between May 17 and 24, 2001. The initial behavior was expected to depend on aircraft characteristics, including physical size of the engines and their position on the airframe and sample details to support these variables were collected concurrently with plume measurements. Initial plume behavior was also expected to vary with atmospheric stability and local wind speed. Dispersion is inherently a random process, so many experimental cases are required to determine the mean behavior and typical variability. This preliminary reporting is based on an analysis of 4138 sweeps, or cross sections, collected at a large North American airport; Los Angeles International Airport (LAX). This study and preliminary report provide new insights into aircraft plume behavior and additional data for more accurate modeling of plume rise and spread. This data set is being further evaluated with the aim of refining these values (e.g., for specific aircraft types) and removing as much conservatism as possible. Additional studies are planned (based on available funding) to analyze potential changes in the derived parameters due to site characteristics (e.g., elevation, weather conditions). The results of these follow-on studies will be separately reported at a later date.

APPROACH

LIDAR (LIght Detection And Ranging) was used in this study to observe the time-varying position and geometry of the jet exhaust. LIDAR is well suited for measuring the geometry of plumes that contain light-scattering particles (aerosols) as the tracer. A LIDAR transmits a pulse of light in a narrow beam and detects the backscatter from light scattering particles as a function of time as the pulse propagates away. The concentration of light scattering particles as a function of range along the pulse's path can be inferred from the time series of detected light intensity. By scanning the LIDAR's pointing direction over a period of time of many LIDAR pulses, the distribution of particles over the region of the sweep (e.g., a vertical plane or plume cross section) can be determined.

Two LIDAR units were used in this research; one using the infrared wavelength and the other using the ultra-violet wavelength. The more successful of the two was OPAL (Ozone Profiling Atmospheric LIDAR) operating at the ultraviolet wavelength of 0.355 µm (after slight modification for this study to measure only aerosol backscatter and not generate the additional wavelengths used to measure ozone). Only the results from this LIDAR (OPAL) are discussed in this paper. Additionally, only one path (or a cross section at one stationary position behind the moving aircraft) is presented due to space restrictions. This path, or horizontal plane of the LIDAR sweep, is shown in Figure 1 as the red line. Additional data reduction would permit data from the infrared scanning LIDAR, which collected data at the other sweep angles shown in Figure 1.

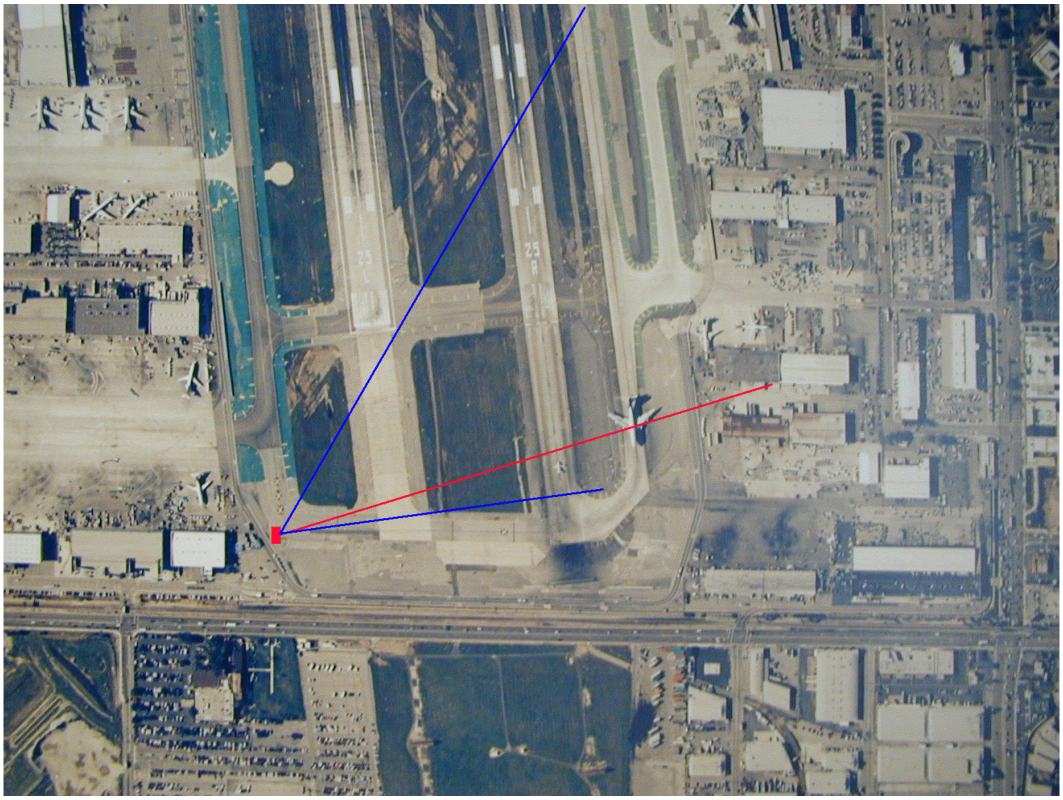

Figure 1: Sweep Angles Of LIDAR Units (Only the Red Sweep is Discussed in This paper)

After data collection, initial quality control measures were performed by NOAA personnel. Computer graphics were then developed and used to evaluate the plume characteristics. Figure 2 shows such an example illustration of a sweep. It can be seen in Figure 2 that the center of the plume can be identified by the area of greatest concentration (red center). This was assumed to represent the height of the plume, or plume rise. For each sweep (cross section) care was taken to carefully determine the height of the center of the plume (Z_{center}), which represents the plume rise.

The outer boundaries of the plume are also easily identified allowing the width and height of the plume to be quantified using normal Gaussian statistics. The outer boundaries of the plume were also carefully determined for each sweep based on the ratio of the concentration. The scale on the side of the chart should also be noted. To make sure that the plume was accurately represented, and not other concentrations or interferences, the plume was only measured to the well-defined boundaries where the Gaussian value was determined for the number of standard deviations from the center of the plume. In the Figure 2 example, this was to the light brown (i.e., 0.54 ρ_{pl} / ρ_{bkg}) fringe as shown.

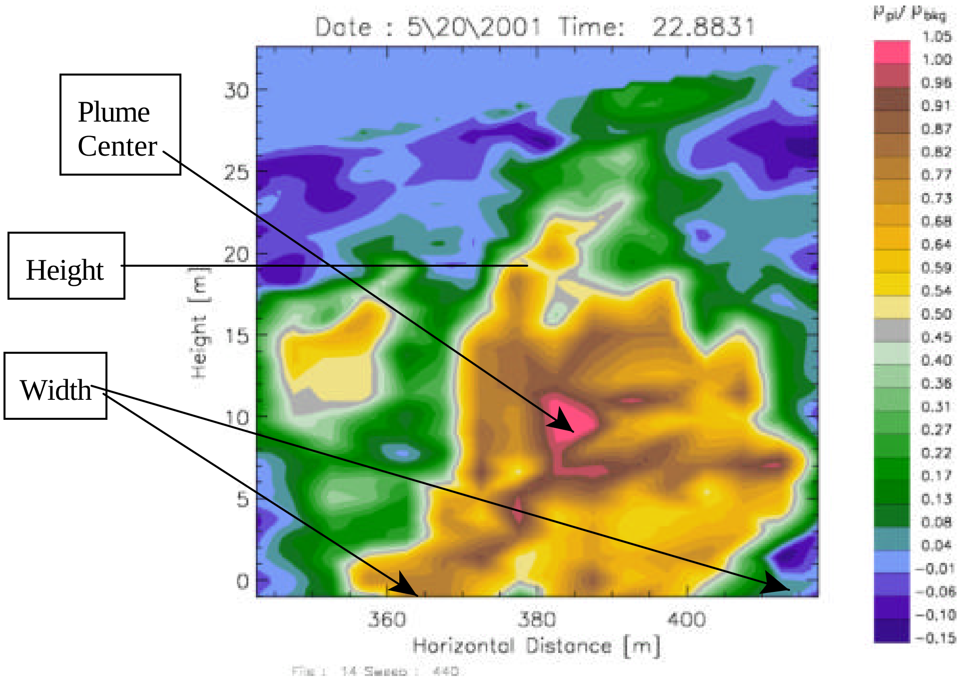

Figure 2. Example of Computer Enhanced LIDAR Image

Using the concept that the scale is the measured density or concentration of aerosol to the background (ρ_{pl} / ρ_{bkg}) the ratio of concentrations from the center (red) to defined outer fringe could be determined since:

$$(\rho_{plc} / \rho_{bkg}) / (\rho_{plf} / \rho_{bkg}) = (\rho_{plc} / \rho_{plf}) \qquad [1]$$

where: ρ_{plc} = density (concentration) of plume center
ρ_{plf} = density (concentration) of plume fringe

Unfortunately, not all sweeps were as easy to determine the center and fringes as the example shown. The example is a well-behaved plume. Plume break-up, multiple centers, high plume rise, and irregular shapes required engineering judgment in many cases. The only way to accurately determine the plume was to review the time series of events (sweeps) behind the aircraft and envision the plume in total. This process was difficult due to the effect of the high velocity jet from the aircraft, which tended to cause irregular mixing and false centers of the actual plume. These data were carefully reduced in such a way to allow for a more systematic recreation of a symmetric plume in the final analysis.

Once the center of the plume and the plume fringe were determined for each sweep used in the analysis, the plume rise for the aircraft event was determined. The plume rise was based on the sweep corresponding to two samples (or sweeps) when the plume had risen to the final measured height with the second greatest height or elevation used in the final plume rise determination. This approach provided a level of conservatism as compared with selecting the sweep with the greatest height or plume rise. A conservative approach was also used to determine the standard deviation of the plume. For the standard deviation determination, the same sweep used for the plume rise was used. The ratio of the concentrations was determined as well as the distance to the fringe from the center of the plume. Using this information, and the basic Gaussian equation, the instantaneous standard deviation was determined. It should be noted that the Gaussian models use time-averaged standard deviations, but the use of multiple aircraft events provide an excellent initial plume spread.

All data was then included in a commercially available spreadsheet and the initial plume parameters derived.

CONCLUSIONS

This is thought to be the first attempt by researchers to characterize the initial plume parameters from jet aircraft using LIDAR. This first analysis was based on all of the useable data collected. From this data (4138 sweeps) events were characterized for each aircraft event. It should be remembered that the second highest value for plume rise was then selected. This resulted in 377 events for large commercial aircraft and 52 events for commuter aircraft.

It can be concluded that significant plume rise occurs. It can also be concluded that initial plume spread is also significant. Findings in this report represent overall values for plume rise and initial plume standard deviations, each derived directly from the measured data. The final, overall values are:

Large Commercial Aircraft (primarily turbofan engines)

Sigma Y = 10.8 meters
Sigma Z = 4.1 meters
Plume Rise = 11.9 meters

Commuter Aircraft (primarily turboprops)

Sigma Y = 10.3 meters
Sigma Z = 4.1 meters
Plume Rise = 12.1 meters

Due to the similarities in these preliminary values, it is recommended that a single set of values be utilized until the additional follow-on analysis is complete. The single set of derived values is as follows:

Sigma Y = 10.5 meters
Sigma Z = 4.1 meters
Plume Rise = 12 meters

This study and preliminary report provide new insights into aircraft plume behavior, and data for more accurate modeling of plume rise and spread. This data set will be further evaluated for the final study report with the aim of refining these values and removing as much conservatism as possible.

For example, the trend of similar results for the larger commercial aircraft and the smaller commuter aircraft was explored in more detail. Figure 3 shows the graphical comparison. The x-axis (abscissa) is the value of the total plume spread while the y-axis (ordinate) is the center of the plume after plume rise has occurred.

It can be seen in Figure 3 that trends are very similar, just as the derived numbers report. However, it is also obvious that many events for the lateral dispersion are greater for the larger commercial aircraft. This result will be further explored by breaking the data into small groups by aircraft types and analyzing the results.

Additional studies also planned (based on available funding) to evaluate potential changes in the derived parameters due to site characteristics, such as elevation and weather. Measurements at other airports are also being considered. These will be topics of follow-on studies.

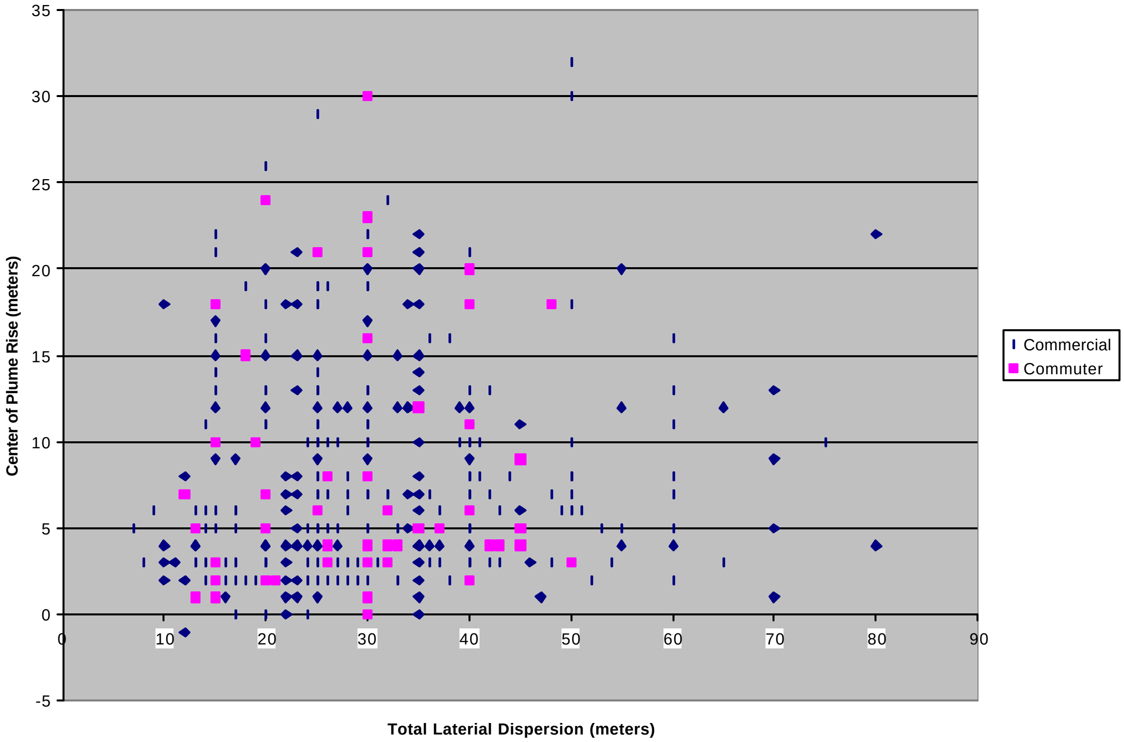

Figure 3. Comparison of Large Commercial and Smaller Commuter Aircraft Trends